Felipe Vannucchi de Camargo
Research Fellow
Dept. of Advanced Mechanics and Materials
Alma Mater Studiorum University of Bologna
Italy

Cristiano Fragassa
Assistant Professor
Department of Industrial Engineering
Alma Mater Studiorum University of Bologna
Italy

Ana Pavlovic
Adjunct Professor
Dept. of Advanced Mechanics and Materials
Alma Mater Studiorum University of Bologna
Italy

Matteo Martignani
Mechanical Designer
Onda Solare Association
Italy

Analysis of the Suspension Design Evolution in Solar Cars

The contrast between modern mobility alternatives and the seek for sustainability has been an essential concern for industry in the last decades, boosted by technologies that have been progressively narrowing this gap. Among them, solar cars represent a contemporary trend to supply this need. Given the complexity embraced by this technology, the attainment of an efficient design demands the improvement of every aspect of the vehicle, including its mechanics. Performing a critical role on the vehicle's stability, the suspension system of solar cars is thoroughly investigated in this work, in particular the evolution of the structural part directly responsible for undertaking the forces subjected to the wheel hub. Three different shapes made out of carbon fiber reinforced plastic are analysed and compared through static and modal finite element analysis: two front forks meant to be coupled to a wishbone joint, and a wheel hub connected to a novel sliding hub system.

Keywords: *Solar vehicles, Suspension, Sliding hub, Carbon fiber, FEM Static Analysis, Modal Analysis.*

1. INTRODUCTION

The main principle promoted by solar vehicles is the possibility to generate energy without harming the environment. However, the constant task of a car to overcoming the inertia provided by surrounding resistances to move makes most of the energy generated by the vehicle to be dissipated through vibrations and motions [1,2]. Hence, the challenge to avoid energy loss is of paramount importance and attaining this premise might be a quite complex engineering endeavour.

To fulfil this goal, all parts of an efficient vehicle must be designed to be as lightweight and resistant as possible [3], while a harmony between their relative movements should be kept to attenuate friction, which is nothing but energy loss sustained by a higher demand on the battery.

The suspension is a vital system of any car for offering stability, safety, vibrations absorption and softening mechanical efforts on other components extending their operational life; hence, enhancing the suspension efficiency is a compelling need if one desires to achieve an efficient vehicle design, especially in solar vehicles where energy management is a particularly important issue [4,5].

Three different wheel support systems, designed by *Onda Solare* Italian designers to meet the technical requirements of three diverse categories of solar cars, are here analysed. The main scope is to characterize their static and dynamic behaviour when mechanically demanded, providing a scientific-based definition on which is the most advantageous design.

Received: October 2016, Accepted: November 2016
Correspondence to: Felipe Vannucchi de Camargo
CIRI Advanced Mechanics and Materials
Alma Mater Studiorum University of Bologna, Italy
E-mail: felipe.vannucchi@unibo.it
doi:10.5937/fmet1703394V

1.1 Solar Car

The solar car concept arose in 1955 with William Coob from General Motors with his exhibition of the "Sunmobile" car in Chicago, introducing the possibility of using photovoltaic cells to convert sun rays into electricity for a car in a time where a diesel-fuelled empire ran the automotive industry supported by powerful oil companies. Even though the non-renewable fuel dependence is still a reality nowadays, the electric vehicles trend has begun to hold its market share powered by the mass-produced pioneer Toyota Prius and more recent alternatives such as the acclaimed Tesla S.

Addressing to foment the progress on solar car technologies, several solar races are held frequently in countries such as Australia, United Arab Emirates, Chile, Belgium and South Africa; encouraging renowned univer–sities and research centres worldwide to prepare for these competitive races while developing novel technologies, promoting popularity, and intensifying industrial attention on this eco-friendly automotive segment.

Given the ongoing perspective and reassuring that this work is up to date, one can highlight that the current champion of the Cruiser category at the most aggressive solar car race, the World Solar Challenge, is studying in the last years how to continually improve the suspension design of their car [6].

Each wheel support was applied on one of the three solar cars considered for this work, all corresponding to a diverse World Solar Challenge (WSC) racing category: Adventure, Challenger and Cruiser (Figure 1), considering 80 kg passengers. Their main differences are displayed in Table 1.

The categories in which each vehicle belongs have some particular characteristics:

- Adventure: is a non-competitive category, aiming at inspiring talented students and engineers to abet the solar vehicles concept;

Figure 1. Solar cars investigated from categories: Adventure (a), Challenger (b) and Cruiser (c)

- Challenger: is the most competitive category and behold the fastest cars with enhanced designs and finest materials on a single stage drive course;
- Cruiser: is also a competitive and new category, based on a regularity trial, aiming at developing novel concepts of transportation and energy efficiency for the next generations of solar cars, encouraging this market segment.

1.2 Suspension

The suspension is certainly one of the most vital systems for the proper car functioning. It is not only responsible for absorbing external vibrations providing comfort to the passengers, but also for shock softening, protecting all the mechanical parts while sustains the entire vehicle weight, maintaining the tires in firm contact with the road enhancing propulsion and safety.

Suspensions can be generally divided into two main groups [7]: dependent and independent. The dependent suspensions have both right and left wheels connected by a transversal trailing rod, so when one of the wheels suffers a vertical displacement (e.g. due to a bump), the other wheel is also affected. On the other hand, the independent suspensions allow vertically autonomous movements for each wheel. The main advantages of the dependent system are low cost and low maintenance while occupying less space; while the independent system leverages are improved steering, handling and comfort.

In solar racing vehicles, there are some preferred suspension designs available. Among them, for offering enhanced steering precision and keeping an adequate camber angle in curves, wishbone connections are widely disseminated either in all wheels of a four-wheeled car, or in the front wheels of a three-wheeled car, which generally considers a trailing arm suspension for the rear wheel. Rear trailing arm suspensions are adopted for conserving energy on bumpy roads once it allows only vertical movements; for offering improved lateral load handling capacity; and diminished bending stresses on suspension components [8].

Still speaking of independent systems, MacPherson is also a common design choice for having a cheap and light design [9], even though its load carrying capacity is relatively low. Both MacPherson [10] and wishbone suspensions [6,11,12] are reported to be used in solar racing cars before. Given the current overview, aside from the wishbone's wheel support evaluation in this study, the analyse of the sliding hub is then particularly relevant due to its innovative feature.

The aforementioned structures are applied in various competitive solar vehicles nowadays, such as the vehicles from the University of Eindhoven, featuring rear trailing arms [6] (Figure 2); the University of New South Wales, with front double wishbones [13] (Figure 3); the University of Johannesburg, with double wishbone suspension composed by composite upright and A-arms [11] (Figure 4); and Stanford with a double wishbone multi-link composition (Figure 5).

The choice for a transversal leaf spring suspension derives from a few important facts for building a competitive solar car: it reduces considerably the unsprung weight; it contributes with less overal weight to the suspension system (considering also the fact that all suspension components for the Cruiser vehicle are made of carbon fiber); and lowering the center of gravity upgrading the stability of the car. Furthermore, similary, non-transversal composite leag springs have already been used in a solar racing car representing good performance and meeting all design requirements [14].

Table 1. Characteristics of the solar cars analysed

Category	*Adventure*	*Challenger*	*Cruiser*
Weight [kg]	260	200	280
Passengers	1	1	4
Total Weight [kg]	340	280	600
Wheels	3	4	4
Approximate dimensions [m]	5.00 x 1.80 x 1.25	4.50 x 1.80 x 1.25	4.65 x 1.80 x 1.30
Cruising Speed [km/h]	51	61	65
Maximum Speed [km/h]	100	120	100
Suspension	Double wishbone (front) and trailing arm (rear)	Double wishbone	Sliding hub

Figure 2. Rear trailing arm suspension by Solar Team Eindhoven [6]

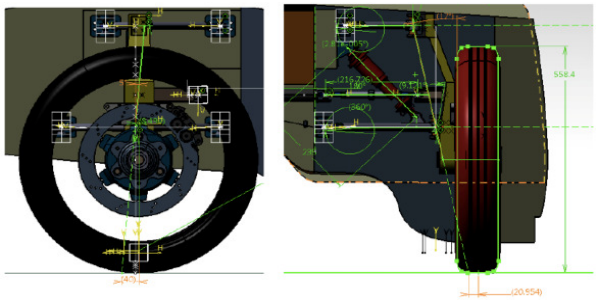

Figure 3. Front double wishbone suspension by Sunswift [13]

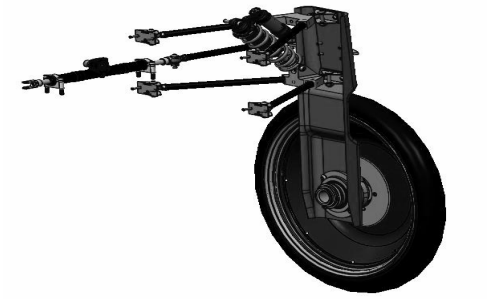

Figure 4. Double wishbone suspension by UJ Solar Car [11]

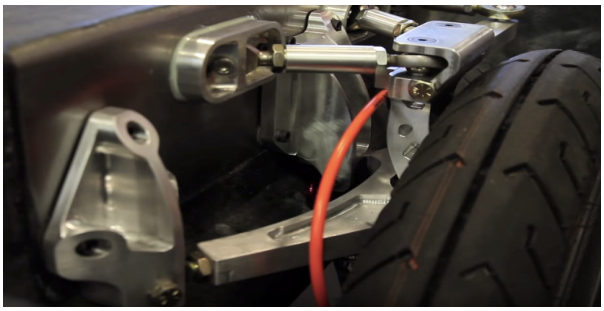

Figure 5. Double wishbone multi-link suspension by the Stanford Solar Car Project

2. MATERIALS AND METHODS

2.1 Wheel Support Designs

In this work, three different designs are considered and compared: two forks that are meant to be coupled with a double wishbone (Figure 6a,b), although their shape and assembly layout is quite distinct, and a new and uncommon wheel hub solution (Figure 6c), all of them connected to a transversal leaf spring. The mounted hubs are shown in Figure 7.

The volumes of the wheel supports are 1340.20 cm^3, 1464.10 cm^3 and 257.35 cm^3 for the Adventure, Challenger and Cruiser cars, respectively; and these geometries are henceforth quoted as A, B and C. The most noticeable difference among these supports, besides the compact size of geometry C, is that each one offers a particular main degree of freedom for absorbing the impact subjected to the vehicle by its own motion:

- Geometry A: Offers a translational displacement normal to the road surface, connected by two ball joints inherent to the wishbone design;
- Geometry B: Also linked by two ball joints, presents, as prominent degree of freedom for undertaking the vertical efforts of the car, a rotation axial to the transversal axis of the vehicle, with a 10^o range;
- Geometry C: Similarly to geometry A, offers a translation to support vertical efforts, although a fixed sliding hub guides it.

As long as every relative movement provided by a mechanical joint involves a certain friction to happen, it is important to underline that this energy spent by a joint, in an electric car, is prevenient from the battery. Thus, the friction involved on every inter-part connection must be decreased to the minimum possible level in order to enhance the energy efficiency.

The novel design of the non-wishbone wheel support studied presents a layout composed by a wheel hub connected to a sliding hub, which is linked directly to the spring, aiming to decrease the energy spent due to friction. It is known that a single ball joint requires less friction than a sliding hub, but the numerous joints that a wishbone design exhibits as a whole makes the alternative of a single sliding surface to become interesting. Besides, this design is more compact and requires a smaller number of parts, also offering weight reduction.

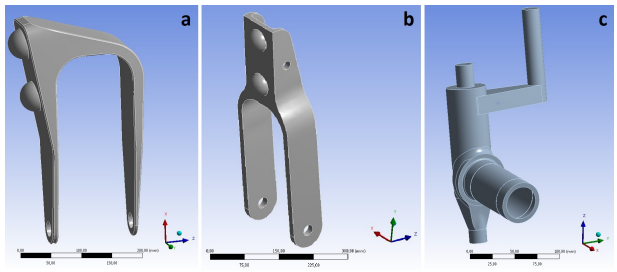

Figure 6. Wheel support geometries for the conventional categories of (a) adventure; (b) challenger; (c) cruiser

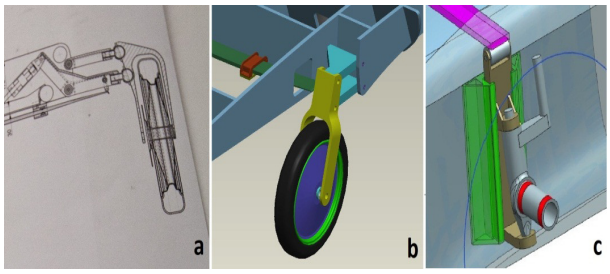

Figure 7. Mounted wheel supports for the conventional categories of (a) adventure; (b) challenger; (c) cruiser

2.2 Carbon Fiber

According to the 21st century demand for novel technologies and products [15] and the aforementioned

current and continuous seek for lightweight resistant materials, fibers and composites are undoubtedly a strong alternative for supplying this demand with successful performance on acute applications [16-19]. In turn, with respect to Carbon Fiber Reinforced Polymers (CFRP) specifically, the application on automotive field is thoroughly consolidated since the Formula 1 pioneering success in 1981, proposing a carbon fiber composite monocoque chassis [20]. Nowadays, in order to enhance resistance, reduce weight, or both, the usage of this composite in basic and structural parts for race cars as well as wholesale vehicles is typical.

The energy efficiency achieved by using such material is especially appealing to solar vehicles [21,22], once their energy source and current conversion technologies require the most efficient solar arrays, batteries, design and materials for achieving a good overall performance. Therefore, once a car with reduced weight would demand less energy to surpass inertia, it is encouraged to widen the usage of composites on structural parts, such as previously implemented suspension components [11].

Apart from the mechanical characteristics, the utilization of carbon fiber is also supported by its recycling possibility [23], once eco-friendly alternatives have been increasingly studied on the composites field [24] due to their large-scale usage and consequent significant environmental impact. Moreover, its safety properties such as gas barrier and flame retardant [25] make the material yet more worthwhile, providing security to vehicles; aspect that might be neglected in some cases despite being of utmost importance [26].

The two forks from geometries A and B and the wheel hub from geometry C were manufactured with pre-impregnated carbon fiber sheets on a temperature-and-humidity-controlled room, followed by an autoclave curing process. As an example, a picture of the manufactured geometry A is shown in Figure 8:

Figure 8. Adventure vehicle's wheel support in carbon fiber

Carbon fiber composites are certainly disseminated by solar car teams throughout the world, mainly based within an epoxy resin matrix, having already provided a weight saving of 55 kg in some vehicles [27]. Furthermore, its application, specifically on a suspension system, does not provide only weight reduction but also increase the safety factor of its components [11].

Actually, the emphasized weight optimization importance for obtaining a good energy efficiency [3] can be quantified: stating as reference a 10% weight reduction, the generated fuel saving for a regular commercial car ranges from 6-8%; the fuel economy on a hybrid vehicle can reach up to 5.1%; and the electric range on an electric car can be improved by 13.7% [28]. Furthermore, a similar study about the weight optimization of suspension knuckle for a solar race car has already been performed [29], and, for this specific case, it was found out that a 452 g weight reduction in the car represents an energy saving as high as 18.6 Wh.

For this work, the composite material considered has an epoxy matrix and a unidirectional T800 carbon fiber reinforcement, by Toray; in which pre-impregnated 0.25 mm thick plies assembled under a $[90/0_3/+45/-45/0_3/90]_s$ orientation result in a variable thickness part (for geometries A and B) and a 5 mm thick part (for C). This configuration is adequate to the effort the wheel hub is subjected, with the longitudinal 0° fibers holding the biggest load share, while the ±45° plies contribute to torsional stiffness and the 90° plies grant a good mechanical resistance in all main directions making a quasi-isotropic material. A fiber volume of 60% was adopted and the composite is considered homogeneous. The density was calculated with the average value of 1.54 g/cm^3, while orthotropic mechanical characteristics and stress limits [30,31] are described in Table 2 for this specific laminate.

In order to point out the reason why carbon fiber is the selected material, the simulations carried in this work were also performed considering aluminium 6151-T6, a common material choice when low cost and light weight are expected, and carbon steel AISI 1040 hot rolled, already used for building wishbone suspension components in other racing car categories [32,33]. Some main properties of aluminium and steel are respectively: Young Modulus of 71 GPa and 200 GPa; Poisson ratio of 0.33 and 0.29; Shear Modulus of 26.7 GPa and 77.5 GPa; and density of 2.77 g/cm^3 and 7.80 g/cm^3 [34,35].

The finite element method (FEM) based analyses of a fiber reinforced composite might be performed by two general approaches [36]: the micromechanical, where it is modeled as a multi-phase composition; and the macromechanical, where the part is treated as an equivalent homogeneous material. Therefore, as this work is based on a preliminary study concerning the global behaviour of the component, the macro-mechanical approach is adopted, which considers a homogeneous anisotropic material. Other researches have already been carried with this same assumption [37,38], specifically for a composite reinforced by a pre-impregnated unidirectional fiber by Toray [36], just like the present work. The adoption of the macro-mechanical premise is actually advised for composite materials which are not solicitated beyond the elastic regime, once until the failure of the first layer, the assemble can be seen as a homogeneous part [30].

Finite element analyses were performed in terms of static and modal studies.

Table 2. Elastic modulus (E) and Shear Modulus (G) [GPa], Poisson ratio, and stress limitis [MPa] for the CFRP laminate

E_1	E_2	E_3	ν_{12}	ν_{23}	ν_{13}	G_{12}	G_{23}	G_{13}	$\sigma_{1,rupture}$	$\sigma_{2,rupture}$	$\sigma_{3,rupture}$	τ_{12}	τ_{12}	τ_{12}
112.5	49	9	0.2	0.25	0.25	13	3.4	3.4	1133	467.5	66	241	100	100

2.3 FEM Static Simulation

The simulations carried to assess the mechanical response of all parts were static once this assumption is proved to grant results faithful to the actual part behaviour [39] and has been widely developed in similar studies [6,31,40,41,].

As for the boundary conditions, given that each wheel hub was applied to a different vehicle with own dimensions and design, the constraints are singular in each case. In all simulations, a force correspondent to the weight of the full car (including 80 kg passengers) divided by the number of wheels under a 3G acceleration was assumed. Also, this acceleration was already set as constraint for vertical forces in an analogous suspension study [42].

While for geometries A and B a frictionless support on the wishbone connection was assumed, a fixed face condition was imposed for geometry C. Besides, a fixed displacement on the axial direction to the wheel was set up for A and B once no movement is allowed in this direction due to the wheel attachment. The boundary conditions are shown in detail in Figure 9. The simulations concern a straight drive condition.

Considering the weight of the car with passengers (Wt) and dividing it by three or four to define the weight applied on each wheel (Ww), the resulting mass was multiplied by the pre defined 3G acceleration. An approximate force (Fw) used in the simulations is stated for each wheel hub as showed in Table 3.

The mesh data is displayed in Table 4, and the meshed geometries are shown in Figure 10.

Table 3. Weight and forces definition

	A	B	C
Wt [kg]	340	280	600
Ww [kg]	114	70	150
Fw [kN]	3.3	2.0	4.4

Table 4. Mesh data

	A	B	C
Nodes	294 025	306 424	114 863
Elements	81 216	78 443	116 353
Element Size [mm]	3	3	2
Average Quality	0.749	0.787	0.977

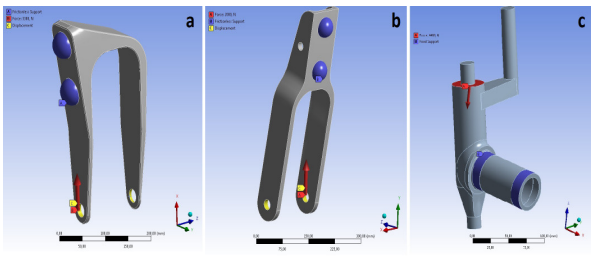

Figure 9. Boundary conditions

The three meshes were discretized by a *hex dominant* method with 3 mm elements for geometries A and B and 2 mm for C once this support is considerably smaller than the others. Also, after preliminary simulations it was noticed that the maximum stress region on geometry C is the fillet. Therefore, a mesh refinement assumption for critical fillet sessions [43] was applied on the fillet and its adjacent faces, based on a size decreasing of the elements in this area aiming to improve simulation accuracy assuming 0.2 mm elements.

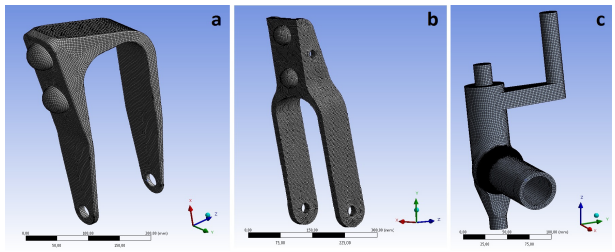

Figure 10. Mesh application

2.4 FEM Modal Analysis

Modal analysis permits to determine the vibration response of a structure in terms of natural frequencies and mode shapes. It is a fundamental step, generally used as starting point for other more detailed dynamic analyses (such as harmonic, dynamic and rigid body motion). It considers that every structure can be subjected to the influence of variable external forces, which in case of their variance in a resonance condition might entail significant wear and durability issues on its mechanical components [44].

Therefore, modal analysis allows the investigation of the dynamic properties of structures subjected to excitation caused by vibrations, aiming to define the resonant frequencies in a way to foresee and avoid the resonance phenomenon by improving the given machine design. This kind of frequency is an outcome caused by the mutual annulment of the stiffness and inertial forces; thus, the source governing the vibration amplitude is damping alone.

For all the endless number of natural frequencies of vibration existent (each one representing a different mode of vibration), the part analysed will suffer a particular deformation, majorly caused either by torsion, or bending, or compression, and so on so forth. Considering the wheel supports investigated and the motion of the car, there are, generally, four types of static load that can be separately or jointly applied to the wheels [45]:

- Lateral Bending: when the vehicle steers a corner in high speed;
- Horizontal Lozenging: due to forward and backward forces applied at diagonally opposite wheels;
- Longitudinal Torsion: Due to bumps simultaneously acting on two diagonally opposite wheels, imposing to the structure a torsion-spring-like solicitation;
- Vertical Bending: basically caused by the car weight from supporting its weight.

Since this work is based on a static analyse representing the mechanical demand on the wheel supports caused by a linear and bumpless motion of the

vehicle, the concern of the modal analysis is to identify the lowest modes of vibration in which the frequencies are able to impose a vertical bending condition to the parts studied.

3. RESULTS AND DISCUSSION

3.1 Static Analysis

The FE static analysis permitted to investigate the stress distributions in respect to the suspensions' wheel supports studied (used for Adventure, Challenger and Cruiser categories) considering different materials (CFRP, aluminium and steel). Maximum stress regions are common in all materials and are shown in Figure 11.

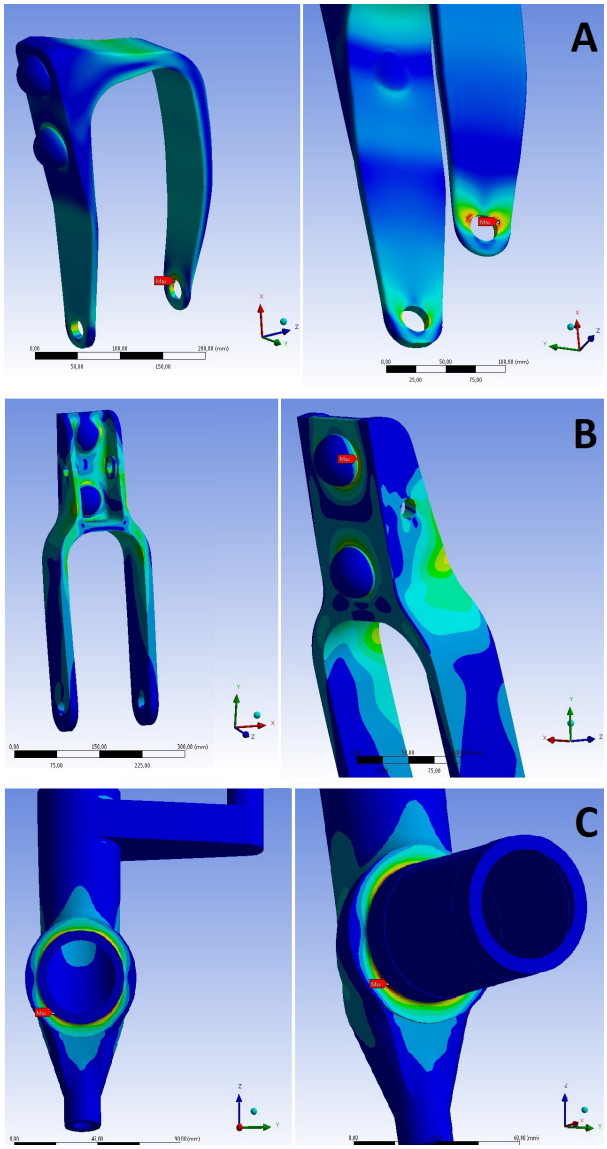

Figure 11. Stress concentrations for the categories of (A) Adventure, (B) Challenger and (C) Cruiser

The maximum stress region on geometry A is the wheel rod attachment hole. Its small dimensions when compared to the whole part coupled with the hole's inherent stress concentration are responsible for this outcome. A similar motorcycle fork-shaped moving arm geometry subjected to its operational efforts has shown to present exactly the same intensified stressed region, validating the result [41].

As for geometry B, a symmetric well-balanced stress gradient is evidenced, with critical region located, naturally, on the wishbone joint. Geometry C shows an accurately symmetric pattern, with severe stress clustering on the fillet.

The Von Mises maximum stress results for both aluminium and steel were exactly the same for each particular support geometry, explained by the fact that the isotropic materials are under the same force and neither reaches the plastic regime. On the other hand, as long as composites are elastic up to their rupture, they do not yield by local plastic deformation such as classical metallic materials. Hence, the elastic limit corresponds to the rupture limit and the safety factor is calculated through the Hill-Tsai method [30].

This criterion states that if its constant (α2) attends to the condition [0 < α2 < 1], the design is safe. For geometries A and B, the 3D Hill-Tsai formula (1) was used since the structures can be considered as solid and were modeled with solid elements. Instead, geometry C, modeled as a shell structure for having a constant thickness and being hollow, has its safety factor calculated by the 2D Hill-Tsai equation (2), which considers only in-plane stresses. For the sake of comparison with the metallic materials, the safety factor of CRFP supports can be calculated according to the expression (3) [30].

$$\alpha^2 = \left(\frac{\sigma_1}{\sigma_{1,rupture}}\right)^2 + \left(\frac{\sigma_2}{\sigma_{2,rupture}}\right)^2 + \left(\frac{\sigma_3}{\sigma_{3,rupture}}\right)^2 - \left(\frac{1}{\sigma^2_{1,rupture}} + \frac{1}{\sigma^2_{2,rupture}} - \frac{1}{\sigma^2_{3,rupture}}\right)\sigma_1\sigma_2 - \left(\frac{1}{\sigma^2_{2,rupture}} + \frac{1}{\sigma^2_{3,rupture}} - \frac{1}{\sigma^2_{1,rupture}}\right)\sigma_2\sigma_3 - \left(\frac{1}{\sigma^2_{3,rupture}} + \frac{1}{\sigma^2_{1,rupture}} - \frac{1}{\sigma^2_{2,rupture}}\right)\sigma_1\sigma_3 + \left(\frac{\tau_{12}}{\tau_{12,rupture}}\right)^2 + \left(\frac{\tau_{23}}{\tau_{23,rupture}}\right)^2 + \left(\frac{\tau_{13}}{\tau_{13,rupture}}\right)^2 \quad (1)$$

$$\alpha^2 = \left(\frac{\sigma_1}{\sigma_{1,rupture}}\right)^2 + \left(\frac{\sigma_2}{\sigma_{2,rupture}}\right)^2 - \left(\frac{\sigma_1.\sigma_2}{\sigma^2_{1,rupture}}\right) + \left(\frac{\tau_{12}}{\tau_{12,rupture}}\right)^2 \quad (2)$$

$$SF = \frac{1}{\alpha} - 1 \quad (3)$$

Finally, Table 5 covers the maximum stress results and safety factors (SF) of all wheel supports. For the metals, safety factor is calculated by the ratio of the Yield Strenght (280 MPa for aluminium and 350 MPa for steel) and the maximum Von Mises stress.

Table 5. Maximum Von Mises stress [MPa] for aluminium or steel, maximum principal stresses for CFRP, and safety factors

	Aluminium and Steel			CFRP							
	Von Mises Maximum Stress	SF Aluminum	SF Steel	σ_1	σ_2	σ_3	τ_{12}	τ_{23}	τ_{13}	α^2	SF CFRP
Adventurer	17	14.7	20.6	15	10	5.2	7	2.7	3	0.013	7.7
Challenger	15	16.7	23.3	36	18	5.5	4.6	4.4	4.4	0.092	2.3
Cruiser	132	1.9	2.6	160	138	-	85	-	-	0.214	1.2

3.2 Modal Analysis

The FE modal analysis allowed the investigation of the dynamic response of the three studied wheel supports. Given the extremely high frequencies encoutered, the analysis is limited to the three first resonant frequencies for each design and material investigated, as displayed in Table 6.

Table 6. Lowest natural frequencies (in Hz) of Adventure (A), Challenger (B) and Cruiser (C) wheel supports as a function of the vibration mode (N)

CFRP

N	A	B	C
1st	70	144	675
2nd	471	312	733
3rd	554	421	1669

Aluminium

N	A	B	C
1st	64	132	618
2nd	430	286	672
3rd	507	384	1528

Steel

N	A	B	C
1st	65	133	617
2nd	435	286	671
3rd	507	387	1529

Table 6 shows that the metallic materials present a very similar behaviour. Figure 13 illustrates this akin resonant trend along the subsequent modes of vibration with the metals curves overlapped and indistinct. Also, it highlights that carbon fiber parts always present higher resonant frequencies for the same vibration mode in a same wheel support design, being therefore a safer material.

In addition, the first resonant frequencies of the suspension part of the Cruiser vehicle are the highest, followed by the Challenger and the Adventure. Thus, the higher the resonance frequency, the more difficult it is to be achieved, and the safer the design. Hence, the analysis is narrowed to carbon fiber, so forth the safest and most lightweight option.

Besides the frequency magnitude, the load type described by each vibration mode is an important matter of concern. For a proper understanding, three axis should be assumed: transversal and longitudinal to the vehicle, and normal to the ground. Table 7 reports all load conditions characterized by the application of a moment in one of the axis in each vibration mode. Figure 12 exhibits the expected not scaled deformations shapes in all cases considering carbon fiber composite as material only.

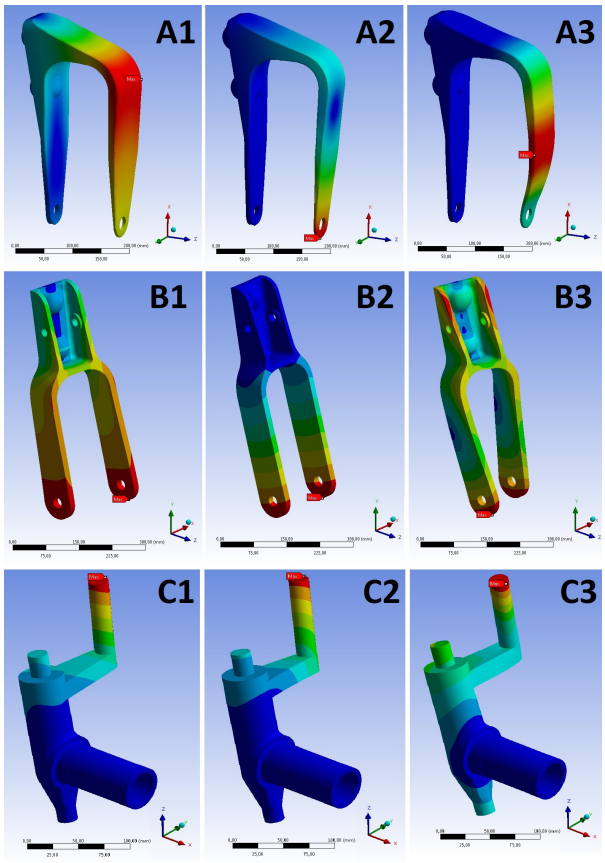

Figure 12. Maximum deformation in first three modes of vibration on (A) Adventure; (B) Challenger; and (C) Cruiser

Table 7. First three modes of vibration and equivalent loads

	A	B	C
f_I [Hz]	70	144	674
$Load_1$	Normal moment	Normal moment	Longitudinal moment
f_{II} [Hz]	471	312	733
$Load_2$	Transversal moment	Transversal moment	Transversal moment
f_{III} [Hz]	554	420	1669
$Load_3$	Longitudinal moment	Normal moment	Normal moment

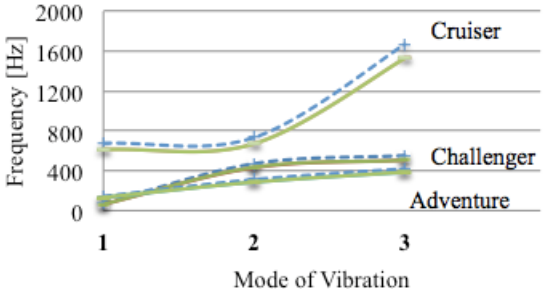

Figure 13. Resonant frequencies for the first three modes of vibration for metals (full line) and CFRP (dash line)

However, as previously stated, the most relevant load type in this study is vertical bending only [45], which is represented by a moment on the transversal axis of the vehicle (Figure 14). Thus, the most relevant results can be narrowed to the lowest vibration mode in which such effort is present (coincidently, all 2nd modes), as displayed in Table 7. Figure 15 shows their respective modal deformation gradient.

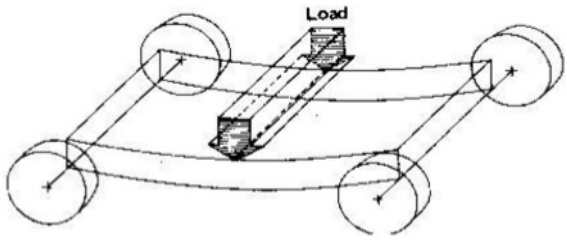

Figure 14. Vertical bending condition [45]

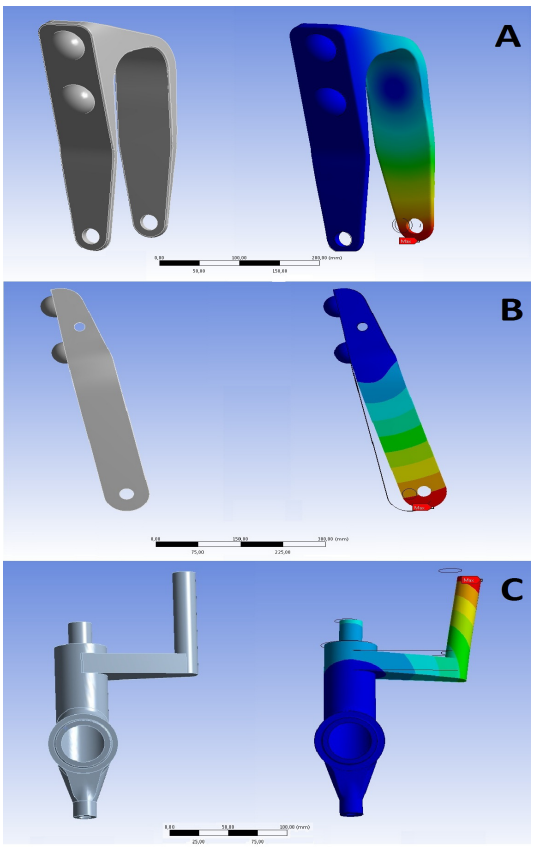

Figure 15. Effect of vertical bending deformation (2nd mode of vibration) on the different suspensions: (A) Adventure; (B) Challenger; and (C) Cruiser

3.3. Weight Comparison

Besides the mechanical response, the weight of the supports is a crucial matter of concern, as explained in previous sessions. Table 8 provides a comparison among all geometries and materials studied.

Table 8. Wheel hub masses

	Mass of each support [kg]		
	A	B	C
CFRP	2.1	2.2	0.4
Aluminium	3.7	4	0.7
Steel	10.5	11.5	2

4. CONCLUSION

Given the current mechanical solicitations, all geometries seem to withstand their operational forces well, hence, failure is not a matter of concern. Also, all designs have high and unattainable resonant frequencies. For example, a racing car equipped with an eight-cylinder internal combustion engine of approximately 750 hp, reaching up to 380 km/h, and all its inherent vibrations, has as parameter the operational frequencies ranging from 0.5 Hz to 20 Hz to grant a trustworthy modal analysis [46]. Thus, the frequency generated by an extremely light electric solar vehicle that achieves up to 120 km/h, is undoubtedly in a safer range of operation.

As for the different geometries, the wheel hubs from the Adventure and Challenger vehicles demonstrated to be safer than the Cruiser in terms of stress concentration and magnitude at operational conditions, although, due to its reduced dimension, the Cruiser support present much higher resonant frequencies being safer in this aspect. Also, the modal results for Adventure and Challenger are validated, since suspension fork structures are known for having their legs as critically affected regions due to bending [47].

On the other hand, regarding the materials, aluminium and steel have static safety factor considerably higher than CRFP, independent of the geometry. However, the modal behaviour of the structures seemed fairly levelled for all materials, being preferably dependent on the part geometry.

From an overall perspective, the suspension parts from the Adventure and Challenger vehicles have showed to be always safer in both analyses made, independently from other factors; while the Cruiser hub is also safe, but significantly less. It is important to emphasize that this difference comes with a cost, and it is caused by a noticeable contrast in weight and dimensions, in which the Cruiser geometry is much more advantageous than others. Also, it is submitted to a considerably higher static load.

Therefore, carbon fiber is undoubtedly the best material for all designs once the resistance is kept at a high level and the weight of the part is significantly decreased, as shown by Table 8. The Cruiser's hub design is also advised as it is the best in terms of energy saving due to its lightweight and low operational friction. Nevertheless, the safety factor presented is seen as safe but insufficient, so a thickness increase made by adding a few carbon fiber plies must be considered aiming to strengthen the part.

The biggest disadvantage of geometry C is that it is designed focusing on a straight wheel drive, not having a steering mechanism as good as A and B's independent wishbone suspension. For the studied solar car project this is not a huge issue because the races in which these vehicles participate, such as in Australia, United States, Chile and Morocco, are predominantly straight. However it is meaningful to emphasize that it would not be the most appropriate design for races held in circuits, such as Suzuka, in Japan.

As long as this work considers solely the effect caused on the suspension by the weight of the car with

passengers on a straight drive assuming a rough road surface; it is encouraged to perform the analysis taking into account more extreme boundary conditions such as turning, in which a force radial to the curve would take place on the part; and emergency breaking, where the inertia of the car movement would turn into an aggravating state of stress on the suspension [47]. Also, the pressure caused by wind on the car might as well be simulated, once considerable wind velocities can be achieved on during solar race events held in deserts such as in Australia and Chile.

ACKNOWLEDGMENT

This research was realized inside the Onda Solare collaborative project, an action with the aim at developing an innovative solar vehicle. The authors acknowledge support of the European Union and the Region Emilia-Romagna (inside the POR-FESR 2014-2020, Axis 1, Research and Innovation)

REFERENCES

[1] Zuo, L., Scully, B., Shestani, J. and Zhou, Y.: Design and characterization of an electromagnetic energy harvester for vehicle suspensions, Smart Materials and Structures, Vol. 19, No. 4, 2010.

[2] Guida, D., Pappalardo, C.M.: A new control algorithm for active suspension systems featuring hysteresis, FME Transactions, Vol. 41, pp. 285-290, 2013.

[3] Taha, Z., et al.: Study of lightweight vehicle vib–ration characteristics and its effects on whole body vibration, in: *Proceeding of the 9th Asia Pacific Industrial Engineering and Management System Conference*, 03-05.12.2008, Bali, pp. 629-633.

[4] Elshafei, M., Al-Qutub, A. and Abdul-Wahid, A.S.: Solar car optimization for the World Solar Challenge, in: *Proceedings of the 13th International Multi-Conference on Systems Signals and Devices*, 21-24.03.2016, Leipzig, pp. 751-756.

[5] Betancur, E., Fragassa, C., et al.: Aerodynamic effects of manufacturing tolerances on a solar car, in: Campana, G. et al. (Ed.): Sustainable Design and Manufacturing, Smart Innovation, Systems and Technologies series, Springer International Publishing AG, 2017. Chapt. 78, pp. 1-9, DOI: 10.1007/978-3-319-57078-5_78

[6] Mathijsen, D.: Redefining the motor car, Rein–forced Plastics, Vol. 60, No. 3, pp. 154-159, 2016.

[7] Gadade, B. and Todkar, R.G.: Design, analysis of A-type front lower suspension arm in commercial vehicle, International Research Journal of Engineering and Technology, Vol. 2, No. 7, pp. 759-766, 2015.

[8] Thosar, A.: Design, analysis and fabrication of rear suspension system for an all terrain vehicle, International Journal of Scientific & Engineering Research, Vol. 5, No. 11, pp. 258-263, 2014.

[9] Purushotham, A.: Comparative simulation studies on MacPherson suspension system, International Journal of Modern Engineering Research, Vol. 3, No. 3, pp. 1377-1381, 2013.

[10] Beres, J.: Sunrunner: the engineering report, Solar Cells, Vol. 31, pp. 425-442, 1991.

[11] Hurter, W.S., van Rensburg, N.J., Madyira, D.M., and Oosthuizen, G.A.: Static analysis of advanced composites for the optimal design of an experimental lightweight solar vehicle suspension system, in: *Proceedings of the ASME International Mechanical Engineering Congress & Exposition*, 14-20.11.2014, Montreal.

[12] Burke, J. et al: Viking XX - Western Washington University's solar race car, Solar Cells, Vol. 31, pp.443-458, 1991.

[13] Paterson, G., Vijayaratnam, P., Perera, C. and Doig, G.: Design and development of the Sunswift eVe solar vehicle: a record-breaking electric car, Journal of Automobile Engineering, Vol. 230, No. 14, pp. 1972-1986, 2016.

[14] Sancaktar, E., Gratton, M.: Design, analysis, and optimization of composite leaf springs for light vehicle applications, Composite Structures, Vol. 44, pp. 195-204, 1999.

[15] Fragassa. C., Pavlovic, A. and Massimo, S.: Using a Total Quality Strategy in a new Practical Approach for Improving the Product Reliability in Automotive Industry, International Journal for Quality Research, Vol. 8, No. 3, pp. 297–310, 2014.

[16] Katsiropoulos, C., Chamos, A., Tserpes, K. and Pantelakis, S.: Fracture toughness and shear behaviour of composite bonded joints based on a novel aerospace adhesive, Composites Part B: Engineering, Vol. 43, No. 2, pp. 240-248, 2012.

[17] Fragassa, C.: Investigations into the degradation of PTFE surface properties by accelerated aging tests, Tribology in Industry. Vol. 38, No. 2, pp. 241-248, 2016.

[18] Giorgini, L., Fragassa, C., Zattini, G., and Pavlovic, A.: Acid aging effects on surfaces of PTFE gaskets investigated by Fourier Transform Infrared Spectroscopy, Tribology in Industry. Vol. 38, No. 3, pp, 286-296, 2016.

[19] Camargo, F.V. et al.: Cyclic stress analysis of polyester, aramid, polyethylene and liquid crystal polymer yarns, Acta Polytechnica. Vol. 56, No. 5, pp. 402-408, 2016.

[20] Tremayne, D.: *The science of formula 1 design: expert analysis of the anatomy of the modern grand prix car*, Haynes Publishing, California, 2011.

[21] Minak, G., Fragassa, C., Camargo, F.V.: A brief review on determinant aspects in energy efficient solar car design and manufacturing. Sustainable Design and Manufacturing 2017, Smart Innovation, Systems and Technologies series. Editors: Campana, G., Howlet, R. J., Setchi, R., Cimatti, B., Springer International Publishing AG, 2017, Chapt. 78, pp: 1-9, DOI: 10.1007/978-3-319-57078-5_76

[22] Camargo, F.V. et al.: Increasing the energy efficiency in solar vehicles by using composite materials in the front suspension, Sustainable Design and Manufacturing 2017, Smart Innovation, Systems and Technologies series. Editors: Campana, G., Howlet, R. J., Setchi, R., Cimatti, B.,

Springer International Publishing AG, 2017, Chapt. 72, pp: 1-11, DOI: 10.1007/978-3-319-57078-5_72
[23] Giorgini. L., Benelli, T., Mazzocchetti, et al: Recovery of carbon fibers from cured and uncured carbon fiber reinforced composites wastes and their use as feedstock for a new composite production, Polymer Composites, Vol. 36, pp. 1084-1095, 2015.
[24] Zivkovic, I., Pavlovic, A., Fragassa, C. and Brugo, T.: Influence of moisture absorption on the impact properties of flax, basalt and hybrid flax/ basalt fiber reinforced green composites, Composites Part B, Vol. 111, pp: 148-164, 2017, DOI: 10.1016 /j.compositesb.2016.12.018.
[25] Elmarakbi, A., Azoti, W.L.: Novel composite materials for automotive applications, in: *Proceedings of the 10th International Conference on Composite Science and Technology*, 02-04.09.2015, Lisboa.
[26] Pavlovic, A. and Fragassa, C.: General considerations on regulations and safety requirements for quadricycles, International Journal for Quality Research, Vol. 9, No. 4, pp. 657–674, 2015.
[27] Tamura, S.: Teijin advanced carbon fiber technology used to build solar car for World Solar Challenge, Reinforced Plastics. Vol. 60, No. 3, pp. 160-163, 2016.
[28] Joost. W.J.: Reducing vehicle weight and improving U.S. energy efficiency using integrated computational materials engineering, Journal of the Minerals, Metals and Materials Society. Vol. 64, No. 9, pp. 1032-1038, 2012.
[29] Betancur, E., Mejia-Gutierrez, R., Osorio-Gomez, G. and Arbelaez, A.: Design of structural parts for a racing solar car, in: *International Joint Conference on Mechanics, Design Engineering and Advanced Manufacturing*, 14-16.09.2016, Catania, pp. 25-32.
[30] Gay, D.: *Materiaux Composites*, Hermes, Paris, 1997.
[31] T800H Technical Data Sheet CFA-007, Toray Carbon Fibers America Inc.
[32] Vivekanandan, N., Gunaki, A., Acharya, C., Gilbert, S. and Bodake, R.: Design, analysis and simulation of double wishbone suspension system, International Journal of Mechanical Engineering, Vol. 2, No. 6, pp. 1-7, 2014.
[33] Deshwal, H., Jangid, R., Mehra, K., Singh, Y., Singh, N., Yadav, N. and Saxena, G.: Finite element analysis and geometric optimization of double wishbone pushrod actuation suspension system of "Supra Saeindia" vehicle, International Journal of Mechanical Engineering, Vol. 3, No. 5, pp. 16-22, 2016.
[34] Metallic Materials and Elements for Aerospace Vehicle Structures Military Handbook. Department of Defense of The United States of America, 1998.
[35] J.E. Shigley and C.R. Mischke: *Mechanical Engineering Design*, McGraw-Hill, New York, 1989.
[36] Ghafarizadeh, S., Chatelain, J.F., Lebrun, G.: Finite element analysis of surface milling of carbon fiber-reinforced composites. International Journal of Advanced Manufacturing Technology, Vol. 87, pp. 399-409, 2016.
[37] Arola, D., Sultan, M.B., Ramulu, M.: Finite element modelling of edge trimming fiber reinforced plastics. Jourmnal of Manufacturing Science Engineering, Vol. 124, No.1, pp. 32-41, 2000.
[38] Soldani, X. et al.: Influence of tool geometry and numerical parameters when modeling orthogonal cutting of LFRP composites. Composites Part A: Applied Science and Manufacturing, Vol. 42, No. 9, pp. 1205-1216, 2011.
[39] Kakria, S. and Singh, D.: CAE analysis, optimization and fabrication of formula SAE vehicle structure, in: *18th Asia Pacific Automotive Engineering Conference*, 10-11.03.2015, Melbourne.
[40] Croccolo, D., Cuppini, R., Vincenzi, N.: Design improvement of clamped joints in front motorbike suspension based on FEM analysis. Finite Elements in Analysis and Design, Vol. 45, pp. 406-414, 2009.
[41] Dhayakar, K., Kamalahar, T., Sakthi, T.V., Manoj, R.S. and Shanmugasundaram, S.: Design and analysis of front mono suspension in motorcycle, Journal of Mechanical and Civil Engineering, Vol. 12, No. 2, pp. 84-100, 2015.
[42] Solanki, V.V. and Patel, N.S.: Rigid body and modal analysis of independent suspension link, International Journal of Thesis Projects and Dissertations, Vol. 2, No. 2, pp. 35-46, 2014.
[43] Awati, P.S. and Judulkar, L.M.: Modal and stress analysis of lower wishbone arm along with topology, International Journal of Application or Innovation in Engineering & Management, Vol. 3, No. 5, pp. 296-302, 2014.
[44] Pavlovic, A., et al.: Modal analysis and stiffness optimization: the case of ceramic tile finishing, Journal of the Serbian Society for Computational Mechanics, Vol. 10, No. 2, pp: 30-44, 2017.
[45] Jain, A.: Computational Analysis and Optimization of Torsional Stiffness of a Formula-SAE Chassis. SAE Technical Paper 2014-01-0355, 2014, doi:10.4271/2014-01-0355.
[46] Kowalczyk, H.: Damper Tuning with the use of a Seven Post Shaker Rig, in: *Proceedings of the SAE 2002 World Congress*, 04-07.03.2002, Detroit.
[47] Croccolo, D., et al.: An analytical approach to the structural design and optimization of motorbike forks. Journal of Automobile Engineering. Vol. 226, pp. 158-168, 2011.

NOMENCLATURE

E_{ijk}	Tensile elastic modulus
G_{ijk}	Shear modulus
A,B,C	Wheel hub geometries
FEM	Finite Element Method
SF	Safety Factor
CFRP	Carbon Fiber Reinforced Polymer
N	Vibration mode number
Wt	Weight of the car with passengers
Ww	Weight applied on each wheel
Fw	Force applied on each wheel
f	Frequency

Greek symbols (Times New Roman 10 pt, bold, italic)

α^2	Hill-Tsai number
σ_{ijk}	Normal stress
τ_{ijk}	Shear stress
υ_{ijk}	Poisson's ratio

Subscripts

1,2,3	Principal directions
I,II,III	Modes of vibration
rupture	Rupture stress

АНАЛИЗА ЕВОЛУЦИЈЕ СИСТЕМА ВЕСАЊА КОД СОЛАРНИХ АУТОМОБИЛЕ

Ф. Де Камарго, К. Фрагаса, А. Павловић, М. Мартињани

Контраст између модерних алтернатива мобилности и потражње одрживости био је битан фактор за индустрију у последњих неколико деценија, подстакнут технологијама које су постепено сужавале ту празнину. Међу њима, соларни аутомобили представљају савремени тренд за обезбеђивање ове потребе. С'обзиром на комплексност ове технологије, постизање ефикасног дизајна захтева побољшање сваког аспекта возила, укључујући његову механику. Критичном улогом у стабилности возила, систем вешања соларних аутомобила је детаљно испитан у овом раду, нарочито еволуција структурног дела која је директно одговорна за подносење сила којима је подвргнута каросерије возила. Три различита облика реализавана од пластике ојачане угљеничним влакнима су анализирана и упоређена статичком и модалном анализом коначних елемената: две предње виљушке спојене у јединствени зглоб, а точак повезан са новим клизним системом.